9-BORAFLUORENES – NMR SPECTROSCOPY AND DFT CALCULATIONS. MOLECULAR STRUCTURE OF 1,2-(2,2′-DIPHENYLYLENE)-1,2-DIETHYLDIBORANE

Bernd WRACKMEYER[1,*], Peter THOMA[2], Rhett KEMPE[3] and Germund GLATZ[4]

Anorganiche Chemie II, Universität Bayreuth, D-95440 Bayreuth, Germany; e-mail: [1] b.wrack@uni-bayreuth.de, [2] peter.thoma@uni-bayreuth.de, [3] kempe@uni-bayreuth.de, [4] germund.glatz@uni-bayreuth.de

Received February 17, 2010
Accepted May 17, 2010
Published online July 29, 2010

Dedicated to Professor Bohumil Štíbr on the occasion of his 70th birthday.

9-Borafluorene derivatives **1** (9-R = Et (**a**), Ph (**b**), Cl (**c**), NEt_2 (**d**)), the pyridine adduct $\mathbf{1py}^+$ and 1,2-(2,2′-biphenylylene)-l,2-diethyldiborane(6) (**3**), were studied by ^{11}B and ^{13}C NMR spectroscopy to obtain a fairly complete data set for the first time. The molecular structure of the doubly hydrogen-bridged 1,2-diphenylenediborane **3** was determined by X-ray diffraction. The gas-phase structures of the compounds **1**, related derivatives, and of some doubly hydrogen-bridged 1,2-diphenylenediboranes were optimized by quantum chemical calculations (B3LYP/6-311+G(d,p) level of theory) and NMR parameters, such as chemical shifts, ^{11}B chemical shift tensors and indirect nuclear ^{13}C–^{11}B spin–spin coupling constants were calculated at the same level of theory and compared with experimental data.
Keywords: 9-Borafluorene; Diborane; NMR; DFT calculation; X-ray diffraction.

Following the pioneering work of Köster[1], 9-borafluorene derivatives have attracted considerable interest in synthesis as well as in theory. The rigid tricyclic planar framework offers the 9-borafluorenyl group as an attractive substituent[2–6]. Recently, the strongly Lewis-acidic perfluorinated 9-borafluorene derivatives[7a,7b] were shown to be promising catalysts in polymerization, e.g. of isobutene[7c]. Similarly, the unusual coordination chemistry of 9-borafluorene derivatives is of interst[7d], as well as related heterocycles derived from 1,8-diborylnaphthalenes[7e,7f]. Moreover, the opening of the 9-borafluorene system towards presumably doubly hydrogen-bridged 1,2-diphenylenediboranes deserves attention[8,9]. The theoretical analysis of molecular 9-borafluorene derivatives and their yet unknown 2,7-polymers suggests remarkable electrooptical properties[10–12], and the isoelectronic re-

Collect. Czech. Chem. Commun. 2010, Vol. 75, No. 7, pp. 743–756

doi:10.1135/cccc2010015

lationship with the important fluorenyl cations[13] is another intriguing subject. The 9-borafluorene moiety has been structurally characterized as a cationic species similar to **1-py**$^+$ with acridine coordinated to boron[3b], in a diborylamine[6], and more recently as the 9-ferrocenyl derivative (**1-Fc**)[14]. However, direct structural information on the doubly hydrogen-bridged 1,2-diphenylenediboranes is almost completely absent. The molecular structure of 1,2:1,2-bis(2,2′-biphenylylene)diborane(6) (**4**) had been given as a figure without crystallographic information[8]. Spectroscopic evidence for 1,2-(2,2′-biphenylylene)diborane(6) (**2**) and 1,2-(2,2′-biphenylylene)-1,2-diethyldiborane(6) (**3**) supports the proposed structures[8,9]. The inspection of all NMR spectroscopic data sets reported so far for 9-borafluorene derivatives, as well as for doubly hydrogen-bridged 1,2-diphenylenediboranes reveals serious gaps with respect to assignment, as well as number of the ^{13}C NMR signals. In contrast, ^{11}B NMR data appear to be complete, except for **1-py**$^+$.

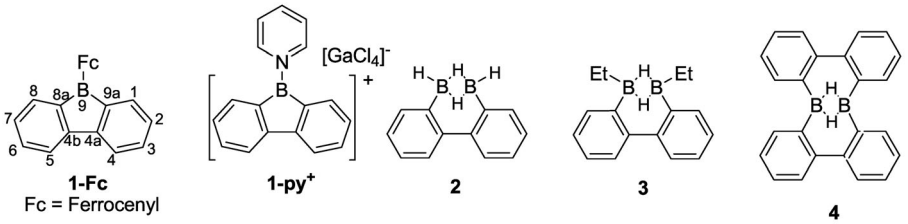

SCHEME 1
An example of a 9-borafluorene derivative **1** [14], the cationic species **1-py**$^+$ [5], and doubly hydrogen-bridged 1,2-diphenylenediboranes **2**–**4**

In the present work, ^{13}C NMR spectra of 9-borafluorene derivatives **1** with various substituents at boron (Et (**a**), Ph (**b**), Cl (**c**), NEt_2 (**d**)) have been measured, the synthesis of **1-py**$^+$ was repeated, and ^{11}B and ^{13}C NMR data were collected. A complete NMR data set was also obtained for **3**, and the molecular structure of **3** was determined by X-ray diffraction. The gas-phase geometries of 9-borafluorene derivatives of type **1**, of compounds related to **1** (cations and dianions), and of the doubly hydrogen-bridged 1,2-diphenylenediboranes **2** and **3** were optimized by DFT methods (B3LYP/6-311+G(d,p) level of theory) and NMR parameters were calculated.

EXPERIMENTAL

All preparative work and the handling of samples were carried out with exclusion of air and moisture, using oven-dried glassware and carefully dried solvents. The compounds studied were prepared following literature methods (**1a** [8], **1b** [7a], **1c** [3], **1d** [3], **3** [8]) and characterized

by their known ^{1}H NMR data sets. NMR spectra (δ, ppm; *J*, Hz) were measured at room temperature in 5 mm o.d. tubes (if not mentioned otherwise) using a Bruker WP 200 and a Varian Inova 400 instruments, equipped with multinuclear units. Chemical shifts are given relatively to $SiMe_4$ ($\delta^{13}C(CDCl_3)$ = 77.0, (CD_2Cl_2) = 53.8, (C_6D_6) = 128.0), F_3B-OEt_2 ($\delta^{11}B$ = 0 for $\Xi(^{11}B)$ = 32.083971 MHz), and neat $MeNO_2$ ($\delta^{14}N$ = 0 for $\Xi(^{14}N)$ = 7.226324 MHz). ^{13}C NMR signals were assigned (except of **1-py**$^+$) using 2D HSQC and HMBC ^{1}H/^{13}C experiments[15].

The calculations were performed using the program package Gaussian 03, revision B.02 [16]. Gas-phase structures were optimized applying DFT hybrid methods (B3LYP)[17] and the 6-311+G(d,p) basis set[18], and the NMR parameters were calculated using the optimized structures at the same level of theory. The optimized structures were confirmed as minima on the respective potential energy surface by the absence of imaginary frequencies. Nuclear magnetic shielding constants $\sigma(^{11}B)$ and $\sigma(^{13}C)$ were calculated by the GIAO method (gauge-including atomic orbitals)[19] and coupling constants by the coupled perturbed DFT methods[20] as implemented in the Gaussian 03 program. Calculated nuclear shielding constants $\sigma(^{11}B)$ and $\sigma(^{13}C)$ were converted to $\delta^{11}B$ and $\delta^{13}C$ data as noted in Table II (footnote *b*) and Scheme 3, respectively.

Pyridine-9-Borafluorenium(1+) Tetrachlorogallate (**1-py**$^+$**[GaCl$_4$]**$^-$)

The synthesis followed essentially the literature procedure[5], starting from a solution of the pyridine adduct of **1c** in CH_2Cl_2 and adding $GaCl_3$ at –78 °C. The reaction mixture was allowed to reach 0 °C, and the red precipitate was filtered off and taken up in CD_2Cl_2 (2 ml) in which it was sparingly soluble at room temperature for the immediate NMR measurements in a 10 mm (o.d.) tube. The broad ^{11}B NMR signal at $\delta^{11}B$ = 57.4 indicated the presence of three-coordinate boron. Although the $^{13}C\{^1H\}$ NMR spectrum was of poor quality, most of the signals could be assigned. Decomposition was indicated by ^{11}B NMR spectra after 1 h, showing a strong signal at $\delta^{11}B$ = 6.5 for the pyridine adduct **1c**-py[3b].

Mixture of Adducts Obtained from the Reaction of **3** with 1,4-Diazabicyclo[2.2.2]octane (DABCO)

A solution of **3** (0.4 g, 1.71 mmol) in toluene (5 ml) was cooled to –30 °C and DABCO (0.2 g, 1.78 mmol) was added in one portion. The mixture appeared to be unchanged (^{11}B NMR) at room temperature. After warming the solution to 60 °C for 15 min, a reaction had taken place to give a mixture containing mainly three adducts (^{11}B and ^{13}C NMR), of which the adduct **5** was the major species. When the toluene was removed, a colorless powder was left (starts to melt at 110 °C), which gave the same ^{11}B NMR spectra (mainly two signals at $\delta^{11}B$ = –2.6 (s) and –2.7 (t, $^1J_{B\text{-}H}$ = 102), when it was re-dissolved in CD_2Cl_2. Signals of minor intensities may be attributed to DABCO-$BEtH_2$ and DABCO-**1a**. Attempts to isolate pure crystalline materials have failed so far.

X-Ray Structural Analyses of the Diborane Derivative **3**

The X-ray crystal structural analysis of **3** was carried out at 133(2) K for a single crystal (selected in perfluorinated oil[21] at room temperature), using a STOE IPDS II (MoKα, 71.069 pm) system equipped with an Oxford Cryostream low-temperature unit. Structure solutions and

refinement were accomplished using SIR97 [22], SHELXL-97 [23], and WinGX [24]. Pertinent data are given in Table I.

CCDC 766359 contains the supplementary crystallographic data for this paper. These data can be obtained free of charge via www.ccdc.cam.ac.uk/conts/retrieving.html (or from the Cambridge Crystallographic Data Centre, 12, Union Road, Cambridge, CB2 1EZ, UK; fax: +44 1223 336033; or deposit@ccdc.cam.ac.uk).

TABLE I
Data pertinent to the crystal structure determination of **3**

Chemical formula	$C_{16}H_{20}B_2$
Molecular weight	233.94 g/mol
Diffractometer	STOE IPDS II; MoKα, λ = 71.073 graphite monochromator
Crystal description	colorless needle
Dimensions	0.59 × 0.21 × 0.19 mm^3
Crystal system	orthorhombic
Space group	*P*2(*1*)2(*1*)2(*1*)
Lattice parameters	*a* = 529.80(6) *b* = 1457.50(14) *c* = 1771.60(18) α = β = γ = 90°
Z	4
Density (calculated)	1.136 g/cm^3
F(000)	504
Measuring range, θ	1.81–25.76°
Absorption coefficient, μ	0.061 mm^{-1}
Radiation type	MoKα
Radiation wavelength, λ	0.71073
Temperature	133(2) K
Reflection unique	2596
Reflection observed [$I > (2\sigma(I)$]	1469
Absorption correction	none (no improvement of parameters)
Refined parameters	171
*R*1[$I > (2\sigma(I)$]; *wR*2 (all data)	0.0627; 0.0840

RESULTS AND DISCUSSION

NMR data of the 9-borafluorene derivatives and of the doubly hydrogen-bridged 1,2-diphenylenediborane **3** are listed in Table II. The observation of the broad ^{13}C(9a) NMR signals, typical of boron-bonded carbon atoms[25], is straightforward, as shown in Fig. 1. It is hard to understand (except for the sparingly soluble **1**-**py**$^+$), why these signals were not reported at all in any of the previous studies. The ^{13}C NMR signal of the quaternary carbon C(4a) is also readily detected, although the position of this particular signal was not mentioned in a more recent paper focusing on this compound[9].

The changes in $\delta^{13}C(1, 3, 4a)$ for the 9-borafluorene derivatives **1** can be compared with those known for $\delta^{13}C$(*ortho*, *para*) of phenylboranes[25,26] bearing comparable substituents at boron, and indicate the π acceptor strength of the three-coordinate boron atom. The $\delta^{13}C(3)$ values should be hardly affected by steric substituent effects, and the deshielding of $^{13}C(3)$ is most pronounced in the case of **1c**, similar to the finding for $PhBCl_2$ [26].

The observation of the broad ^{13}C(B-C) NMR signals is not only important for a complete structural assignment. The broadening $\Delta\nu_b(^{13}C)$ of these ^{13}C(B-C) NMR signals reveals information on unresolved (partially relaxed) scalar ^{13}C–^{11}B spin–spin coupling which can readily be extracted[27] if $\Delta\nu_b(^{13}C)$, as described by $T_2^{SC}(^{13}C)$, is mainly related to scalar relaxation of the second kind[28], dependent on the quadrupolar relaxation time $T^Q(^{11}B)$ (Eq. (*1*), with $I(^{11}B) = 3/2$ and $T^Q(^{11}B) = [\pi h_{1/2}(^{11}B)]^{-1}$).

$$\Delta\nu_b(^{13}C) = (4/3)\pi\ 3/2(3/2 + 1)\ [J(^{13}C,^{11}B)]^2\ [T^Q(^{11}B)] \qquad (1)$$

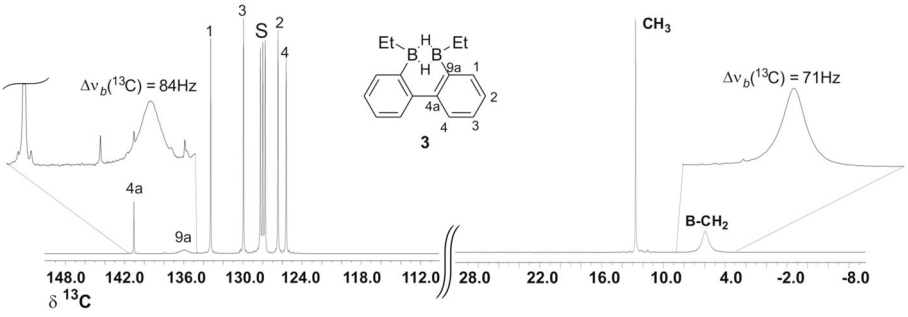

FIG. 1
100.3 MHz $^{13}C\{^1H\}$ NMR spectrum of the diborane(6) derivative **3** (at 23 °C; ca. 5% in C_6D_6 (S)). Note the broad ^{13}C(9a) and $^{13}C(BCH_2)$ NMR signals. Assignment was achieved by 2D HMQC and HSQC $^1H/^{13}C$ experiments

TABLE II
^{11}B and ^{13}C NMR parameters[a,b] of 9-borafluorene derivatives

Compd.	$\delta^{13}C$							$\delta^{11}B$
	C(9a)	C(4a)	C(1)	C(2)	C(3)	C(4)	B–R	
1a R = Et	142.2 (br) $\Delta\nu_b(^{13}C)$ = 44 Hz [62.0] {62.1}	155.8	134.7	129.2	135.9	120.4	16.0 (br), 10.2 $\Delta\nu_b(^{13}C)$ = 33.5 Hz [54.0] {55.4}	73.1 $h_{1/2}$ = 435 Hz {72.1}
1b R = Ph	143.0 (br)	155.1	136.4	129.2	135.5	120.5	139.0 (br) (*i*), 133.9 (*o*), 128.3 (*m*), 132.0 (*p*)	64.5 {63.6}
1c R = Cl	139.5 (br) $\Delta\nu_b(^{13}C)$ = 61 Hz [75.0] {76.2}	153.4	133.0	129.3	136.9	120.7	–	62.1 $h_{1/2}$ = 460 Hz {64.7}
1d R = NEt_2	141.5 (br)	151.4	130.1	129.2	132.5	120.2	45.1 16.7	38.5 {38.9}[c]
1-py^{+} [d]	n.o. (low solubility)	157.5	134.0	131.0	143.5	123.0	145.0, 129.0, 148.0	57.4 {57.1}
3 R = Et	135.9 (br) $\Delta\nu_b(^{13}C)$ = 84 Hz [54.4] {67.3}	141.1	133.3	126.5	130.0	125.6	6.0 (br), 12.7 $\Delta\nu_b(^{13}C)$ = 71 Hz [59.2] {58.6}	19.4 $h_{1/2}$ = 247 Hz {17.4}
5 [e]	156.0 (br)	152.2	134.0	128.8	128.2	121.2	11.6 (br), 12.3, 9.7 (br), 14.8	–2.7 –2.6

[a] Measured at 23 °C in $CDCl_3$ (**1**), C_6D_6 (**3**) and CD_2Cl_2 (**1-py**$^{+}$, **5**); br, broadening owing to partially relaxed one-bond ^{13}C–^{11}B spin–spin coupling; $\Delta\nu_b(^{13}C)$, see the text; $h_{1/2}$, full line width at half height of the ^{11}B NMR signal. [b] Coupling constants $^{1}J(^{13}C,^{11}B)$ calculated (Eq. (*1*)) are given in brackets; quantum chemically calculated NMR data (coupling constants $^{1}J(^{13}C,^{11}B)$ and $\delta^{11}B$) are given in braces. Nuclear shielding constants $\sigma(^{11}B)$ were converted into $\delta^{11}B$ data with reference to $\sigma(^{11}B, B_2H_6)$ = 84.1 and $\delta^{11}B(B_2H_6)$ = 18. [c] Calculated for R = NMe_2. [d] $\delta^{14}N$ = –175 ($h_{1/2}$ > 1 kHz). [e] $\delta^{13}C(NCH_2)$ = 49.1, 48.3; other NCH_2: 48.5, 52.7.

Thus, from experimental data such as the line widths $h_{1/2}(^{11}B)$ of the ^{11}B NMR signals and $\Delta\nu_b(^{13}C)$, the magnitude of $^nJ_{C\text{-}B}$ can be calculated, and some values for $n = 1$ are given in Table II. These data are in the expected range, in agreement with the results of quantum chemical calculations (*vide infra*).

Some aspects of the reactivity of **3** have been reported[8,9]. The reversible opening of the B–C_{Ar} bond in **3** to give **1a** and 1,2-diethyldiborane(6) is an important observation[8]. Here, we report that **3** reacts with bases in a similar way. Upon gentle heating with DABCO, the adduct **5** is formed along with minor amounts of the symmetrical adducts **6** and **7** (Scheme 2).

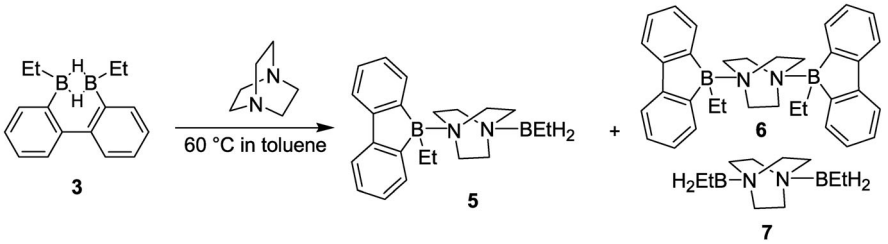

SCHEME 2
Reaction of **3** with 1,4-diazabicyclo[2.2.2]octane (DABCO)

*X-ray Structural Study of the 1,2-(2,2′-Diphenylylene)-1,2-diethyldiborane (**3**)*

The molecular structure of the diborane derivative **3** is shown in Fig. 2. The stacking of the molecules (Fig. 3) explains the orientation of the ethyl groups in the solid-state structure which differs from that found for the optimized calculated gas-phase structure (*vide infra*). The intermolecular distance between the best planes of the tetracyclic structure is 340.2 pm. Distances B–C_{Ar} (157.5 and 156.5 pm) are comparable with those in triphenylborane (158.9 and 157.1 pm)[29], although the boron atoms in **3** possess a coordination number > 3. The mean distance B–C_{ethyl} (157.7 pm) is very close to the values found for triethylborane (157.5, 157.3, 157.2 pm)[30] and slightly longer than that of B–C in bis(9-borabicyclo[3.3.1]nonane) (156.5 pm)[31]. Although there are only few accounts of solid-state structures of diborane(6) derivatives[8,31–35], it becomes apparent that the B–B distances change from about 175 pm [33] (in the parent diborane(6) B_2H_6 176 ± 1 pm [31]; see also ref.[36] for the electron diffraction study of 1,2-dimethyldiborane(6)) to 185.6 pm [35], including 183.9 pm for **3** in the present work. The effect of the fairly large distance B–B in **3** is mirrored by the slight deviation from a coplanar arrangement of the phenyl groups. They are twisted against each

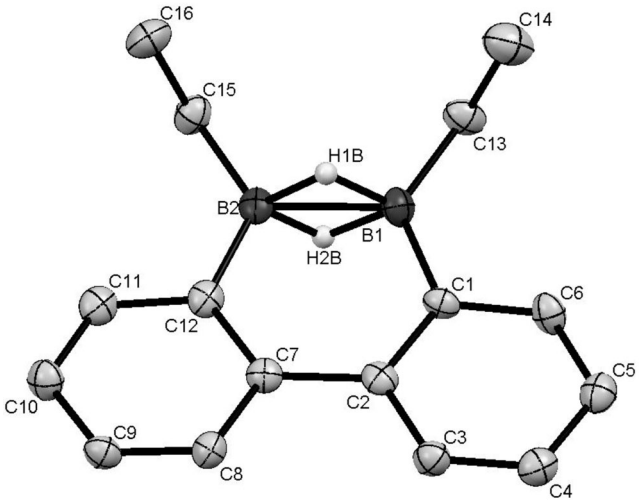

FIG. 2

Molecular structure of **3** (ORTEP, 40% probability; hydrogen atoms except of B–H have been omitted). Selected bond lengths (in pm) and angles (in °): B1–B2 183.9(4), B1–C1 157.5(5), B2–C12 156.5(6), B1–C13 156.7(5), B2–C15 158.7(5), C13–C14 153.4(6), C15–C16 153.6(5), C2–C7 149.5(4), C1–C2 141.5(5), C2–C3 140.7(5), C3–C4 137.7(5), C4–C5 139.2(5), C5–C6 137.9(6), C6–C1 139.9(5), C7–C8 141.2(5), C8–C9 138.1(5), C9–C10 139.4(5), C10–C11 138.0(5), C11–C12 139.6(5), C12–C7 143.9(5); C1–B1–B2 111.8(3), B2–B1–C13 122.4(3), C13–B1–C1 125.7(4), C12–B2–C15 123.9(3), C15–B2–B1 122.2(3), B1–B2–C12 113.8(3), B1–C1–C2 124.7(3), B2–C12–C7 123.3(3), C1–C2–C7 123.4(4), C12–C7–C2 122.8(4), B1–C13–C14 112.5(3), B2–C15–C16 112.1(3)

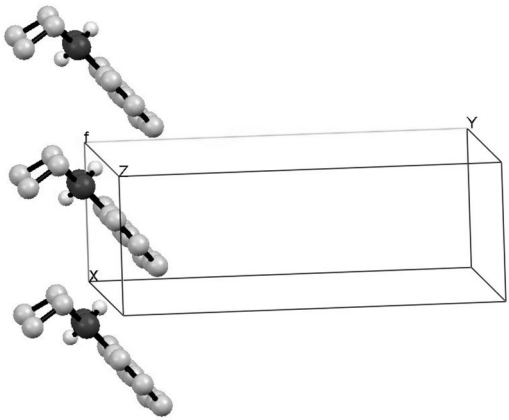

FIG. 3

View of molecules of **3** in the crystal lattice, showing the stacking and the orientation of the B–Et groups

other by 3.8°, apparently in order to avoid close contacts between the C(3)–H and C(8)–H units opposite to the boron atoms.

DFT Calculations for 9-Borafluorene Derivatives and Doubly Hydrogen-Bridged 1,2-Diphenylenediboranes

In previous studies[10–12], DFT calculations aimed for a description of the electronic structure of 9-borafluorene derivatives. Here, we have used the optimized geometries (throughout at the B3LYP/6-311+G(d,p) level of theory) to calculate ^{11}B NMR parameters (^{11}B nuclear shielding[35] and one-bond ^{13}C–^{11}B spin–spin coupling constants[36,37]; see Table II). The calculated data for the 9-borafluorene derivatives and the diborane(6) derivative **3** agree reasonably well with experimental data. Calculated $\delta^{13}C$ values (not given in Table II) show a small error of < 3.5 ppm for all aromatic ^{13}C nuclei, taking the shielding constant $\sigma(^{13}C, C_6H_6)$ as a reference. Some species were included (Scheme 3), not yet characterized experimentally, such as the cation **8**, 9-*H*-9-borafluorene **9** and its dianion **10**. The increase in nuclear

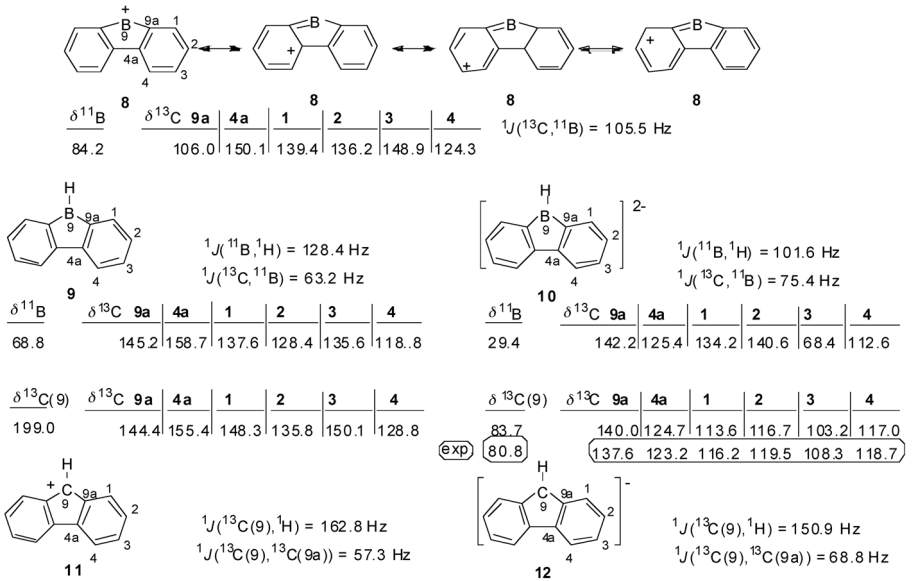

SCHEME 3

Calculated NMR parameters of the cation **8**, 9-*H*-9-borafluorene **9**, its dianion **10**, the isoelectronic fluorenyl cation **11**, and the fluorenyl anion **12** (exp. data from ref.[42]). Nuclear shielding constants $\sigma(^{13}C)$ were converted into $\delta^{13}C$ data with reference to $\sigma(^{13}C, C_6H_6) = 49.7$ and $\delta^{13}C(C_6H_6) = 128.5$)

shielding of $^{13}C(9a)$ in the cation **8** with a bond angle of 130.5° at the boron atom reminds of the situation in allenes, since the C–B–C unit in **8** is comparable to a strained allene. As indicated in Scheme 3, the positive charge should be delocalized, and therefore, the nuclear shielding in particular of $^{13}C(3,6)$ is markedly decreased. The surroundings of these carbon atoms are least affected by structural changes. In any case, this cation is an elusive species, and all attempts to detect it[3b,8] have not been successful. However, adducts of **8** are known[3b], in which the boron atom is three-coordinate, such as in **1-py**$^+$. The experimental NMR data obtained here (Table II) agree reasonably well with those calculated. In the case of the dianion **10**, the derivative **1b(LiOEt$_2$)$_2$** has been studied by ^{11}B and, in part, by ^{13}C NMR (without assignment) in solution[7a]. Of other comparable derivatives, bearing bulky groups at boron and some of the ring carbon atoms, the ^{11}B NMR data are known, also some ^{13}C NMR data (again without assignment), and even the solid-state structures were determined, showing the coordination of the lithium atoms to the dianion[40,41]. The calculated $\delta^{11}B$ data of free $[\mathbf{1b}]^{2-}$ ($\delta^{11}B$ = 17.2) differs significantly from the experimental value for **1b(LiOEt$_2$)$_2$** in THF ($\delta^{11}B$ = 6.3 [7a]). The calculated $\delta^{11}B$ = 9.9 for **1b(LiOH$_2$)$_2$** as a model compound comes closer to the experimental value.

Therefore, the calculated $\delta^{11}B$ and $\delta^{13}C$ data for free dianions such as **10** (Scheme 3) are not directly comparable with experimental data. However, the trend of the calculated coupling constants $^1J_{C\text{-}B}$ and $^1J_{B\text{-}H}$ in going from neutral "antiaromatic" **9** to the "aromatic" dianion **10** is instructive. The magnitude of $^1J_{B\text{-}H}$ becomes smaller, in agreement with the negative charge, whereas that of $^1J_{C\text{-}B}$ increases, indicating the increased B–C bond order in the "aromatic" ring system. The analogous trend is found for the respective coupling constants $^1J_{C\text{-}C}$ and $^1J_{C\text{-}H}$ in the fluorenyl cation **11** and fluorenyl anion **12**. In the latter, the calculated $\delta^{13}C$ data are close to experimental data. This indicates that interactions with the counterion are expectedly weaker for the monoanion **12** than for the dianion **10**.

Although there are very few experimental determinations of the ^{11}B chemical shift tensor for three-coordinate boron[43], the data appear to be reproduced by calculations with sufficient accuracy[44], to allow for a meaningful discussion. Examples are given in Table III. Figure 4 shows the orientation of the principal axes of the ^{11}B chemical shift tensor components in the plane of the molecules. The magnetic field B_0-induced rotation of charge about the δ_{11} and δ_{22} axes involve particularly magnetic dipole allowed σ–π or σ–π^* electronic transitions, whereas the rotation of charge

about the δ_{33} axis (perpendicular to the molecular plane) concerns σ–σ* transitions which are less deshielding owing to their greater difference in energy. Clearly, changes in the components δ_{11} and δ_{22} reflect σ and π effects, whereas δ_{33} is more sensitive to σ effects, e.g. as a result of electronegative groups at boron[42] (see the data for **1-py**$^+$ in comparison with the isoelectronic **1b** or **1c** and $C_{12}H_8B$-NH_2).

Finally, the comparison of the optimized gas-phase structure of **3** with some results of the crystal structure determination deserves a comment. The optimization starting from the solid-state structural parameters did not lead to a minimum. Instead, a minimum was found for the *trans*-positions

TABLE III
Calculated components of the ^{11}B nuclear shielding tensor in 9-borafluorenes and triphenylborane, converted to δ_{11}, δ_{22}, and δ_{33}

Compound		δ_{11}	δ_{22}	δ_{33}	$\delta^{11}B$ (iso)
$C_{12}H_8B$–R	No.				
R = H	**9**	104.6	95.7	6.4	68.9
R = Me		121.2	87.0	8.1	72.1
R = Et	**1a**	120.5	85.9	9.4	71.9
R = Ph	**1b**	92.0	87.0	11.9	63.6
BPh_3		94.6	94.6	1.6	63.6
R = py	**1py**$^+$	100.2	41.2	29.8	57.1
R = Cl	**1c**	92.2	75.8	26.1	64.7
R = NH_2		64.5	48.5	7.0	40.0
R = NMe_2		63.1	38.9	14.8	38.9

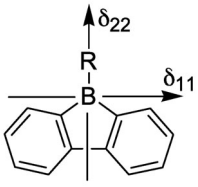

FIG. 4
Proposed orientation of the ^{11}B chemical shift tensor (δ_{33} axis is perpendicular to the molecular plane). The shift component δ_{22} lies along the C_2 symmetry axis. See Table III for data

of the ethyl groups. The calculated distance B–B (180.5 pm) is somewhat shorter than the experimental value. The calculated structure (Fig. 5) shows that the planes of the phenyl groups are twisted against each other by about 9°. In contrast, calculated optimized gas-phase structures, in which the ethyl groups are replaced by methyl groups (in **3**) or by hydrogen (in **2**), show that the phenyl groups are exactly in one plane, in accord with shorter calculated distances B–B (179.8 pm for the B–Me derivative and 176.0 pm for **2**)

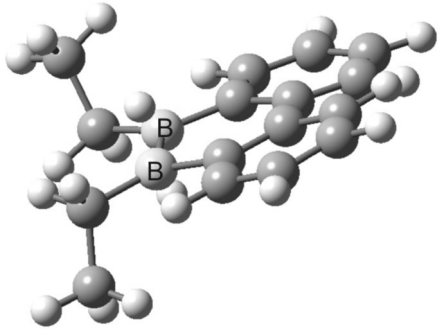

FIG. 5
Calculated optimized gas-phase structure of **3**, showing the ethyl groups in *trans*-positions and the mutual twisting of the phenyl groups

CONCLUSIONS

Changes in ^{13}C chemical shifts of 9-borafluorenes reflect π acceptor properties of the electron deficient boron atom. In principle, this is also true for ^{11}B chemical shifts, although the calculation of the ^{11}B chemical shift tensor shows that the substituent effects are a complex mixture of π and σ interactions with the group directly linked to the boron atom. Altogether, NMR parameters of 9-borafluorenes, for which a fairly complete data set has been obtained in this work, are well reproduced by quantum chemical calculations, at least as long as the gas-phase structures of isolated molecules or ions are comparable with the solution-state structures. The crystal structure determination of 1,2-(2,2′-biphenylylene)-1,2-diethyldiborane(6) (**3**) confirms unambiguously the doubly hydrogen-bridged structure. Stacking of the molecules in the crystal lattices enforces an orientation of the B–ethyl groups which is unfavorable in the gas phase.

REFERENCES

1. Köster R., Benedikt G.: *Angew. Chem.* **1963**, *75*, 419.
2. Köster R., Benedikt G., Fenzl W., Reinert K.: *Liebigs Ann. Chem.* **1964**, *702*, 197.
3. a) Narula C. K., Nöth H.: *J. Organomet. Chem.* **1985**, *281*, 131; b) Narula C. K., Nöth H.: *Inorg. Chem.* **1985**, *24*, 2532.
4. van Veen R., Bickelhaupt F.: *J. Organomet. Chem.* **1973**, *47*, 33.
5. Gross U., Kaufmann D.: *Chem. Ber.* **1987**, *120*, 991.
6. Männig D., Nöth H., Prigge H., Rotsch A.-R., Gopinathan S., Wilson J. W.: *J. Organomet. Chem.* **1986**, *310*, 1.
7. a) Romero P. E., Piers W. E., Decker S. A., Chau D., Woo T. K., Parvez M.: *Organometallics* **2003**, *22*, 1266; b) Piers W. E., Irvine G. J., Williams V. C.: *Eur. J. Inorg. Chem.* **2000**, 2132; c) Lewis S. P., Chai J., Collins S., Sciarone T. J. J., Henderson L. D., Fan C., Parvez M., Piers W. E.: *Organometallics* **2009**, *28*, 249; d) Bontemps S., Bouhadir G., Miqueu K., Bourissou D.: *J. Am. Chem. Soc.* **2006**, *128*, 12056; e) Hoefelmeyer J. D., Sole S., Gabbai F. P.: *Dalton Trans.* **2004**, 1254; f) Gabbai F. P.: *Angew. Chem., Int. Ed.* **2003**, *42*, 2218.
8. Köster R., Willemsen H. G.: *Liebigs Ann. Chem.* **1974**, *704*, 1843.
9. Hong H., Chung T. C.: *J. Organomet. Chem.* **2004**, *689*, 58.
10. Briere J.-F., Cote M.: *J. Phys. Chem. B* **2004**, *108*, 3123.
11. Chen R.-F., Zheng C., Fan Q.-L., Huang W.: *J. Comput. Chem.* **2007**, *28*, 2091.
12. Thanthiriwatte J. S., Gwaltney S. R.: *J. Phys. Chem. A* **2006**, *110*, 2434.
13. Olah G. A., Prakash G. K. S., Liang G., Westerman P. W., Kunde K., Chandrasekhar J., Schleyer P. v. R.: *J. Am. Chem. Soc.* **1980**, *102*, 4485.
14. Kaufmann L., Vitze H., Bolte M., Lerner H.-W., Wagner M.: *Organometallics* **2008**, *27*, 6215.
15. Berger S., Braun S.: *200 and More NMR Experiments*, Wiley-VCH, Weinheim, 2004.
16. Frisch M. J., Trucks G. W., Schlegel H. B., Scuseria G. E., Robb M. A., Cheeseman J. R., Montgomery J. A., Jr., Vreven T., Kudin K. N., Burant J. C., Millam J. M., Iyengar S. S., Tomasi J., Barone V., Mennucci B., Cossi M., Scalmani G., Rega N., Petersson G. A., Nakatsuji H., Hada M., Ehara M., Toyota K., Fukuda K., Hasegawa J., Ishida M., Nakajima T., Honda Y., Kitao O., Nakai H., Klene M., Li X., Knox J. E., Hratchian H. P., Cross J. B., Adamo C., Jaramillo J., Gomperts R., Stratmann R. E., Yazyev O., Austin A. J., Cammi R., Pomelli C., Ochterski J. W., Ayala P. Y., Morokuma K., Voth G. A., Salvador P., Dannenberg J. J., Zakrzewski V. G., Dapprich S., Daniels A. D., Strain M. C., Farkas O., Malick D. K., Rabuck A. D., Raghavachari K., Foresman J. B., Ortiz J. V., Cui Q., Baboul A. G., Clifford S., Cioslowski J., Stefanov B. B., Liu G., Liashenko A., Piskorz P., Komaromi I., Martin R. L., Fox D. J., Keith T., Al-Laham M. A., Peng C. Y., Nanayakkara A., Challacombe M., Gill P. M. W., Johnson B., Chen W., Wong M. W., Gonzalez C., Pople J. A.: *Gaussian 03*, Revision B.02. Gaussian, Inc., Pittsburgh (PA) 2003.
17. a) Becke A. D.: *J. Chem. Phys.* **1993**, *98*, 5648; b) Lee C., Yang W. R., Parr R. G.: *Phys. Rev. B* **1988**, *37*, 785; c) Stephens P. J., Devlin F. J., Chablowski C. F., Frisch M. J.: *J. Phys. Chem.* **1994**, *98*, 11623.
18. a) McLean D., Chandler G. S.: *J. Chem. Phys.* **1980**, *72*, 5639; b) Krishnan R., Binkley J. S., Seeger R., Pople J. A.: *J. Chem. Phys.* **1980**, *72*, 650.
19. Wollinski K., Hinton J. F., Pulay P. J.: *J. Am. Chem. Soc.* **1990**, *112*, 8251.

20. Helgaker T., Jaszunski M., Pecul M.: *Prog. Nucl. Magn. Reson. Spectrosc.* **2008**, *53*, 249.
21. Kottke T., Stalke D.: *J. Appl. Crystallogr.* **1993**, *26*, 615.
22. Altomare A., Burla M. C., Camalli M., Cascarano G. L., Giacovazzo C., Guagliardi A., Moliterni A. G. G., Polidori G., Spagna R.: *J. Appl. Crystallogr.* **1999**, *32*, 115.
23. Sheldrick G. M.: *SHELX97, Program for Crystal Structure Analysis* (Release 97-2). Institut für Anorganische Chemie der Universität Göttingen, Göttingen 1998.
24. Farrugia L. J.: *J. Appl. Crystallogr.* **1999**, *32*, 837.
25. Wrackmeyer B.: *Prog. Nucl. Magn. Reson. Spectrosc.* **1979**, *12*, 227.
26. Odom J. D., Moore T. F., Goetze R., Nöth H., Wrackmeyer B.: *J. Organomet. Chem.* **1979**, *173*, 15.
27. Mlynárik V.: *Prog. Nucl. Magn. Reson. Spectrosc.* **1986**, *18*, 277.
28. Abragam A.: *The Principles of Nuclear Magnetism*, pp. 305–315. Oxford University Press, Oxford 1961.
29. Zettler F., Hausen H. D., Hess H.: *J. Organomet. Chem.* **1974**, *72*, 157.
30. a) Boese R., Blaeser D., Niederprüm N., Nüsse M., Brett W. A., Schleyer P. v R., Bühl M., van Eikema Hommes N. J. R.: *Angew. Chem.* **1992**, *104*, 356; b) Boese R., Blaeser D., Niederprüm N., Nüsse M., Brett W. A., Schleyer P. v R., Bühl M., van Eikema Hommes N. J. R.: *Angew. Chem., Int. Ed. Engl.* **1992**, *31*, 314.
31. Brauer D. J., Krüger C.: *Acta Crystallogr., Sect. B: Struct. Crystallogr. Cryst. Chem.* **1973**, *29*, 1684.
32. Smith H. W., Lipscomb W. N.: *J. Chem. Phys.* **1965**, *43*, 1060.
33. Al-Juaid S. S., Eaborn C., Hitchcock P. B., Kundu K. K., Molla M. E., Smith J. D.: *J. Organomet. Chem.* **1990**, *385*, 13.
34. Wehmschulte R. J., Diaz A. A., Khan M. A.: *Organometallics* **2003**, *22*, 83.
35. Mennekes T., Paetzold P., Boese R.: *Angew. Chem., Int. Ed. Engl.* **1990**, *29*, 899.
36. Hedberg L., Hedberg K., Kohler D. A., Ritter D. M., Schomaker V.: *J. Am. Chem. Soc.* **1980**, *102*, 3430.
37. a) Bühl M. in: *Encyclopedia of Computational Chemistry*, (P. v. R. Schleyer, Ed.), Vol. 3, pp. 1835–1845. Wiley, Chichester 1999; b) Bühl M., Schleyer P. v. R.: *J. Am. Chem. Soc.* **1992**, *114*, 477.
38. Wrackmeyer B., Berndt A.: *Magn. Reson. Chem.* **2004**, *42*, 490.
39. a) Wrackmeyer B., Tok O. L.: *Z. Naturforsch., B: Chem. Sci.* **2005**, *60*, 259; b) Wrackmeyer B.: *Z. Naturforsch., B: Chem. Sci.* **2005**, *60*, 955; c) Wrackmeyer B., Klimkina E. V.: *Z. Naturforsch., B: Chem. Sci.* **2008**, *63*, 923; d) Wrackmeyer B., García Hernández Z., Lang J., Tok O. L.: *Z. Anorg. Allg. Chem.* **2009**, *635*, 1087.
40. Grigsby W. J., Power P. P.: *J. Am. Chem. Soc.* **1996**, *118*, 7981.
41. Wehmschulte R. J., Khan M. A., Twamley B., Schiemenz B.: *Organometallics* **2001**, *20,* 844.
42. Browne S. E., Asher S. E., Cornwall E. H., Frisoli J. K., Harris L. J., Salot E. A., Sauter E. A., Trecoske M. A., Veale P. S., Jr.: *J. Am. Chem. Soc.* **1984**, *106*, 1432.
43. a) Bryce D. L., Wasylishen R. E., Gee M.: *J. Phys. Chem. A* **2001**, *105*, 3633; b) Forgeron M. A. M., Bryce D. L., Wasylishen R. E., Rösler R.: *J. Phys. Chem. A* **2003**, *107,* 726.
44. Sefzik T. H., Turco D., Iuliucci R. J.: *J. Phys. Chem. A* **2005**, *109*, 1180.